Oxidative dehydrogenation of a biomass derived lignan – Hydroxymatairesinol over heterogeneous gold catalysts

Olga A. Simakova [a,d], Elena V. Murzina [a], Päivi Mäki-Arvela [a], Anne-Riikka Leino [b], Betiana C. Campo [a], Krisztián Kordás [b], Stefan M. Willför [c], Tapio Salmi [a], Dmitry Yu. Murzin [a,*]

[a] Laboratory of Industrial Chemistry and Reaction Engineering, Process Chemistry Centre, Åbo Akademi University, FI-20500 Åbo/Turku, Finland
[b] Microelectronics and Materials Physics Laboratories, EMPART Research Group of Infotech Oulu, University of Oulu, FI-90014 Oulu, Finland
[c] Laboratory of Wood and Paper Chemistry, Process Chemistry Centre, Åbo Akademi University, FI-20500 Åbo/Turku, Finland
[d] Graduate School of Materials Research, Åbo Akademi University, Porthansgatan 3-5, FI-20500 Åbo/Turku, Finland

ARTICLE INFO

ABSTRACT

Synthesis of the lignan oxomatairesinol via oxidative dehydrogenation of the naturally occurring lignan hydroxymatairesinol was studied over gold catalysts supported on C, TiO_2, SiO_2, Al_2O_3, and MgO. In order to investigate the reaction performance over the gold catalyst, synthesis of lignan oxomatairesinol was carried out in different organic solvents/water mixtures under synthetic air and nitrogen atmosphere at 373 K, and using also isolated hydroxymatairesinol isomers as a starting material. The results were compared with those obtained over palladium catalysts. Synthesized supported gold catalysts as well as the corresponding supports were characterized by TEM, XRD, ICP-OES, CO_2-TPD, FTIR (using pyridine as a probe molecule), and XPS. Gold catalysts were shown to display superior performance compared with palladium ones: the activity was 4 times higher, with selectivity toward oxomatairesinol being 100%, while 60–85% were obtained over palladium catalysts. In contrast to palladium, the activity of gold catalysts is high in aerobic conditions and water–propan-2-ol mixture. However, activity and selectivity of gold catalysts were shown to be dependent on the electronic state of the metal and, similar to palladium catalysts, on the support acidity.

1. Introduction

Lignans are natural phenolic compounds found in different parts of plants, such as wooden parts, roots, leaves, stem, seeds, flowers, and fruits. However, plants mainly contain lignans in small amounts, moreover, usually as glycosidic conjugates that are associated with fiber components, making the isolation process complicated [1]. Flax seed, sesame seed, and rye grains are among the richest known food sources of lignans. Coniferous trees contain a large number of different lignans in unconjugated form. The type and amount of lignan depend on the species and part of the tree. Thus, Norway spruce (*Picea abies*) knots contain large amounts of lignans: α-conidendrin (Coni), todolactol A derivatives, secoisolariciresinol, lariciresinol, pinoresinol, matairesinol (MAT), isolariciresinol, α-conidendric acid (ConiA), lignan A, isohydroxymatairesinol, and hydroxymatairesinol (HMR) [2–4]. The latter is the most abundant one, constituting 65–85 wt.% of the total lignans and occurs in unconjugated free form [5].

Lignans are known as human health-promoting agents. A lignan-rich diet, for example, decreases the risk for various cancers and cardiovascular diseases [6]. Besides the anticarcinogenic effects, lignans are proven to have antioxidative effects [7–9]. Studies of the lignans matairesinol (MAT) and oxidized MAT (oxoMAT) for radical and superoxide scavenging activities have shown that MAT has the highest radical scavenging activity while oxoMAT exhibits the highest superoxide scavenging activity.

Lignans or lignan derivatives, due to their antioxidative activity [10] and UV-protection properties [11], can be applied for cosmetic and pharmaceutical uses (skin- and hair-care products), as well as color-keeping agents for textile industry, wherein the active agent is selected from the group consisting of hydroxymatairesinol (HMR), lariciresinol, secoisolariciresinol, isolariciresinol, oxomatairesinol (oxoMAT), α-conidendrin (Coni), liovil, picearesinol, syringaresinol, and nortrachelogenin. Among this group of lignans, only HMR can be extracted in considerable amounts from the Norway spruce (*Picea abies*) knots, while oxoMAT cannot be obtained in large quantities from natural resources.

Several valuable lignans have been synthesized using HMR as a starting material [12,13]. For instance, MAT can be produced through hydrogenolysis of HMR (K-acetate adduct of HMR) under hydrogen pressure over Pd/C catalyst in dichloroethane and in ethanol by using Raney-Nickel or Pd/C catalysts [14,15]. Another lignan that is of interest is oxoMAT, which can be obtained through

oxidative dehydrogenation of HMR. The formation of oxoMAT from HMR by light-irradiation was reported in [16], while in [17], 2,3-dichloro-5,6-dicyano-1,4-benzoquinone (DDQ) was used as an oxidizing agent. An attempt has been made over Pd/C to perform the reaction via heterogeneous catalysis, providing a more commercially attractive synthesis of oxoMAT. Unfortunately, oxoMAT was not the only product in this reaction [18]. There is no additional information available about this synthesis carried out over heterogeneous catalysts. Hence, the need for industrially applicable catalytic methods for the selective synthesis of lignan oxoMAT (oxomatairesinol) exists.

In this paper, a new approach for oxoMAT synthesis utilizing heterogeneous Au catalysts is reported. The obtained data were compared with the results over heterogeneous Pd/C catalysts, which are also active in this reaction. OxoMAT was obtained via oxidative dehydrogenation of HMR, and the reaction network is presented in Scheme 1.

The lignan HMR exists in nature as a mixture of two diastereomers of HMR: (7R,8R,8'R)-(-)-7-allo-hydroxymatairesinol (HMR 1) and (7S,8R,8'R)-(-)-7-allo-hydroxymatairesinol (HMR 2), which can be isomerized into each other. The ratio between HMR 2/HMR 1 is typically equal to 2. Both HMR 1 and HMR 2 can be transformed by oxidative dehydrogenation to oxoMAT.

In this study, the activity of gold catalysts, the influence of catalyst support, solvent, and reaction atmosphere were investigated in oxidative dehydrogenation of hydroxymatairesinol.

2. Experimental section

2.1. Catalysts

2.1.1. Palladium catalysts

Two powdered Pd catalysts were utilized in HMR oxidation: Pd/Sibunit prepared by the authors (denoted as Pd/C) and a commercial one 5 wt.% Pd/C (Degussa).

Carbon supported palladium catalysts were prepared by using deposition of Pd(II)-hydroxochlorocomplexes in the amounts corresponding to the final metal loading (4 wt.%). Support was impregnated with Na_2CO_3 aqueous solution at pH = 8; thereafter, palladium precursor H_2PdCl_4 (10^{-3} M) aqueous solution was added dropwise in the ratio corresponding to Na:Pd = 21 mol/mol as described in [19], followed by drying of the catalyst at 353 K in air overnight and reduction under flowing hydrogen at 423 K. Meso-

porous carbon material Sibunit (S_{BET} = 450 m^2/g, micropore area 37.7 m^2/g, average pore diameter 9 nm) was used as a support.

Palladium on activated carbon catalyst (Degussa) was dried overnight at 353 K and then reduced under flowing hydrogen at 423 K.

2.1.2. Gold catalysts

Several methods of catalyst preparation have been applied: direct ion exchange (DIE) of the gold species with the hydroxyl groups of the support surface as described in [20] and deposition–precipitation with urea (DPU) [21]. Carbon supported gold catalysts were prepared via the immobilization of PVA stabilized gold sols by the carbon support (Sibunit) [22]. The detailed procedures are given below.

2.1.2.1. Au/Al₂O₃ preparation by direct ion exchange (DIE).
Hydrogen tetrachloroaurate (HAuCl₄ 99.9% ABCR, Darmstadt) was diluted with deionized water up to the concentration of 5·10^{-4} M in the amount corresponding to the final Au loading of 2 wt.%. The solution was heated up to 343 K and powdered Al₂O₃ (UOP, A-201, S_{BET} = 200 m^2/g) was added. The slurry was mixed for 1 h, washed with ammonium hydroxide (4 M) for 1 h, dried overnight at 353 K, and calcined in air at 573 K for 4 h. The obtained catalyst was marked as Au/Al₂O₃-DIE.

2.1.2.2. Au/Al₂O₃, TiO₂, SiO₂, MgO preparation by deposition–precipitation with urea (DPU).
An aqueous solution of HAuCl₄ with the concentration of 5 × 10^{-4} M in the amount corresponding to the final Au loading of 2 wt.% was mixed with urea (Sigma–Aldrich, 99.5%). The amount of urea was calculated to achieve the concentration of 0.21 M. The solution was heated up to 354 K and then the powdered supports such as Al₂O₃ (UOP, A-201, S_{BET} = 200 m^2/g), TiO₂ (Degussa AG, Aerolyst 7708, anatase >70%, S_{BET} = 45 m^2/g), SiO₂ (Merck, S_{BET} = 480–540 m^2/g), and MgO (Sigma–Aldrich, 99%) were added. The slurry was mixed for 24 h at 354 K and then filtered, washed with water, dried overnight at 353 K, and calcined at 573 K for 4 h. The catalyst supported on alumina was denoted as Au/Al₂O₃-DPU to distinguish it from a catalyst prepared by direct ion exchange.

2.1.2.3. Au/C preparation by gold sols immobilization by carbon.
HAuCl₄ (99.9% ABCR, Darmstadt) was dissolved in deionized water up to a concentration of 60 µg/ml. While maintaining this
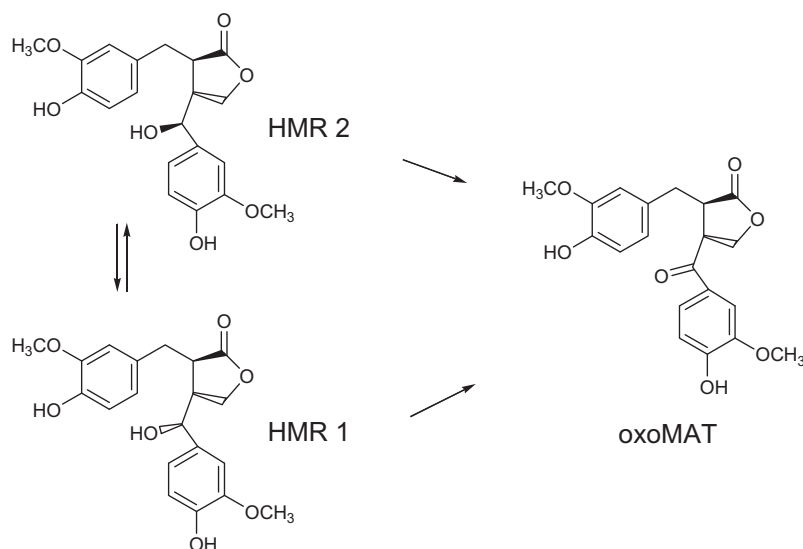
Scheme 1. Reaction pathway of lignan hydroxymatairesinol (HMR) transformations over heterogeneous gold catalysts.

solution under vigorous stirring, 2 wt.% solution of PVA was added at Au/PVA weight ratio equal to 1:5. Freshly prepared 0.1 M solution of $NaBH_4$ was added dropwise at $Au/NaBH_4$ weight ratio equal to 1:100. Within a few minutes of sol generation, the sol was immobilized by adding mesoporous carbon material Sibunit (S_{BET} = 450 m^2/g, micropore area 37.7 m^2/g, average pore diameter 9 nm). The nominal metal loading was 2.5 wt.%. After 2 h, the slurry was filtered and the catalyst was washed thoroughly with deionized water, followed by drying overnight at 333 K in air.

2.2. Catalyst characterization

2.2.1. Metal particle size determination

X-ray diffraction experiments were performed by using CuKα radiation (Siemens D5000 diffractometer equipped with a graphite monochromator to suppress fluorescent and Cu-Kβ radiation). The average crystallite size of the gold catalyst particles was estimated using Scherrer's equation from the peak half-widths of Au(1 1 1) reflection measured at $2\Theta \sim 38.3°$. Instrumental broadening and unresolved CuKα1 and α2 radiation were neglected (error less than 2%).

Electron microphotographs of the samples were taken by a LEO 912 OMEGA energy-filtered transmission electron microscope by using 120 kV acceleration voltage. Histograms of the particle size distribution were obtained by counting at least 100 particles on the micrographs for each sample.

2.2.2. Gold metal loading analysis

The metal loading was determined by inductively coupled plasma-optical emission spectroscopy (ICP-OES) in a PerkinElmer, Optima 5300 DV spectrometer. For that purpose, 60 mg of the sample was treated with 4 ml of aqua regia, digested in a microwave oven, diluted to 100 ml, and analyzed by spectrometer.

2.2.3. XPS study of the metal oxidation state

The XPS measurements were carried out in a PHI Quantum 2000 Scanning ESCA Microprobe spectrometer with Al anode. Gold supported on TiO_2, Al_2O_3, and SiO_2 was analyzed as powder mounted in a double sided adhesive tape. The survey and multi spectra were collected at 187.75 eV and 11.75 eV pass energy, respectively. During the analyses, electron and ion beams were applied over the catalyst to compensate the charge effect. Spectra deconvolution was performed with the free software XPS Peak 4.1. A combination of 30% Lorentzian and 70% Gaussian curves was fitted after subtraction of a Shirley background. For quantitative analysis, the peaks areas were affected for the correspondent sensitivity factors.

2.2.4. Support basicity measurements

Magnesia, titania, and alumina basicity was measured by temperature-programmed desorption of CO_2 (CO_2-TPD) by using Micromeritics AutoChem 290. Measurements were performed in a conventional flow-through reactor with CO_2 as the probe molecule. Two hundred and fifty milligram of metal oxide was flushed with a stream of helium (100 ml/min) to clean the sample at 823 K for 30 min before cooling to 323 K. A stream of CO_2 was allowed to saturate the solid particles for 30 min, and weakly bound CO_2 and other physisorbed molecules were removed by a stream of pure He for 1 h. Chemisorbed CO_2 was desorbed by heating to 1173 K (ramp of 10 C/min), while He was used as a carrier gas. The effluent from the reactor was analyzed by a TC detector. CO_2 calibration was performed by pulse injection of 1 ml CO_2 to determine the actual amount of CO_2 desorbed from the magnesia.

2.2.5. Support acidity measurements

The acidity of the supports was determined by Fourier transformed infrared spectroscopy (FTIR) using pyridine as a probe molecule. Thin self-supporting wafers of the adsorbents were prepared by pressing and placed in the cell. The cell was evacuated to $\sim 10^{-6}$ Torr at 723 K for 1 h. Thereafter, the cell was cooled to 373 K, and background (Bkg) spectra were taken as an average of accumulated 100 scans over the frequency range (4000–400 cm^{-1}). Pyridine was than adsorbed onto the sample at 373 K for 30 min. The subsequent desorption was performed at 523 K, 623 K, and 723 K. The spectra were taken between each temperature ramp at 373 K. Adsorption bands around 1610 and 1450 cm^{-1} were characterizing Lewis acid sites, while the adsorption signals at 1545 and 1630 cm^{-1} were corresponding to the Brønsted acidity of the adsorbent [23].

2.3. Hydroxymatairesinol (HMR) oxidation to oxomatairesinol (oxoMAT)

2.3.1. Starting material

Hydroximatairesinol was isolated from Norway spruce knots as described in [24]. Lignan was extracted from ground knots by acetone–water mixture. The extract was concentrated in a rotary evaporator and then purified by flash chromatography. Two diastereomers of HMR: (7R, 8R, 8'R)-(-)-7-allo-hydroxymatairesinol (HMR 1) and (7S, 8R, 8'R)-(-)-7-allo-hydroxymatairesinol (HMR 2) were obtained as a mixture with the ratio between them HMR 2:HMR 1 = 2:1 mol/mol. The purity of HMR was determined by GC to be 95%. The major contaminant was the lignan conidendrin and conidendric acid (see Fig. 1).

Both isomers HMR 1 and HMR 2 could be oxidized, and the isomerization between them occurs. For the experiments, the obtained mixture containing isomers at the ratio of HMR 2:HMR 1 = 2 mol/mol was utilized as a reactant. However, to study each isomer activity in the oxoMAT synthesis, HMR 1 (92% of purity) and HMR 2 (85% of purity) were used as starting materials. The separation of the isomer from the mixture was performed by flash chromatography.

2.3.2. Oxidation/dehydrogenation of hydroxymatairesinol

The reaction was performed under atmospheric pressure in a stirred 200 ml glass reactor, equipped with a heating jacket (using silicon oil as the heat transfer medium), a reflux condenser (cooling medium set 253 K), oil lock, pitched-blade turbine, and stirring baffles. In a typical experiment, 250 mg of catalyst was put into reactor in case of gold catalysts and 100 mg in case of palladium. To study the support activity, 245 mg of alumina was charged into the reactor. The catalyst grain size was 45–63 μm to suppress the internal mass transfer limitations. Furthermore, the reaction mixture was stirred at 1000 rpm to avoid external mass transfer limitations, and the experiments were performed in the kinetic regime. The catalysts were preactivated in situ by heating under hydrogen (AGA, 99.999%) flow (100 ml/min) until 393 K, and thereafter, the reactor was cooled down to the reaction temperature 343 K under
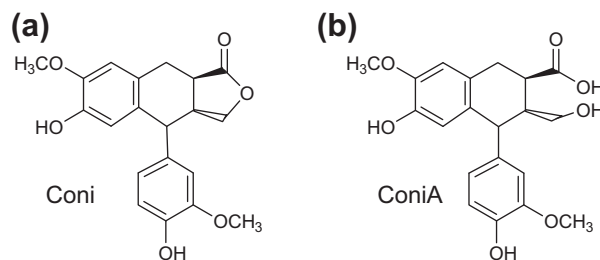
Fig. 1. Structure of lignan: (a) α-conidendrin (Coni); (b) α-conidendric acid (ConiA).

nitrogen (AGA, 99.999%) flow (100 ml/min). To perform the reaction over palladium catalysts, propan-2-ol (Sigma–Aldrich, 99.8%) was used as a solvent. Gold catalysts were studied in different solvents and their mixtures with deionized water (Table 2). The following organic solvents: ethanol (Altia Corporation, 99.5%), propan-2-ol (Sigma–Aldrich, 99.8%), butan-1-ol (Acros, 99%), pentan-2-ol (The British Drug Houses Ltd., 95%), cyclohexanol (J.T. Baker, 99%), 1,4-Dioxane (Labscan, 99.8%), and tetrahydrofuran (THF) (Labscan, 99.8%), mixed with water were applied as solvents as well. The reactant solution (100 ml) with an HMR concentration of 1 mg/ml was poured into the reactor. The gas flow was changed to synthetic air, except the case of dehydrogenation *per se* over palladium and gold catalysts, where the reaction was performed under nitrogen flow. The stirring was started at reaction time set to zero and the first sample was withdrawn.

2.3.3. Product analysis

Samples were withdrawn from the reactor at different time intervals and analyzed by gas chromatography (GC) using a HP-1 column (length 25 m, inner diameter 0.20 mm, film thickness 0.11 μm) and a flame ionization detector (FID) operating at 573 K. For the analysis, 100 μl (concentration of 1 mg/ml) of the sample was taken and 2 ml of the internal standard for the GC containing mainly betulinol (0.02 mg/ml) and C21:0 fatty acid (0.02 mg/ml) dissolved in methyl *tert*-butyl (MTBE, $C_5H_{12}O$) was added. Samples were placed in a water bath at 313 K, where the MTBE and solvent were evaporated in a stream of nitrogen. Thereafter, the samples were dried in an oven at 313 K under vacuum for 20 min. The prepared samples were silylated prior to the analysis as follows: dried samples were dissolved in the silylation mixture of 80 μl N,O-bis(trimethylsilyl)trifluoroacetamide (BSTFA, 98%, Fluka), 25 μl trimethylchlorsilane (TMCS, 98%, Acros Organics), and 25 μl pyridine (99.0%, J.T. Baker). The samples were kept at 343 K for 40 min and transferred to vials and then analyzed by GC. One microliter of the silylated sample was injected with an autosampler. The injection temperature was 533 K and the split ratio was 1:20. Hydrogen served as a carrier gas. The initial temperature of the column was 393 K (for 1 min), and the temperature was increased at a rate 6 K/min to 573 K (for 10 min). The peaks were identified by analysis with a gas chromatograph–mass spectrometer operating at the same GC conditions.

3. Results and discussion

3.1. Catalysts properties

3.1.1. Au and Pd particle size and metal loading

Characterization data confirmed that gold particles were successfully deposited as nano-particles in case of all utilized supports. The obtained TEM images and XRD patterns are shown in Fig. 2, where d is an average metal particle size.

Gold particles supported on titania, silica, alumina, and mesoporous carbon Sibunit have maxima in the particle size distribu-

Table 2
The effect of solvent on the activity and selectivity in HMR oxidative dehydrogenation. Experiments were performed over 250 mg 2 wt.% Au/Al_2O_3 (DIE), HMR concentration was 1 mg/ml, the total volume of solution was 100 ml.

Solvent	Selectivity toward OxoMAT, %	Conversion after 4 h, %	Activity, $\times 10^5 \times$ mol/ l $\times$ sec $\times g_{cat}$	pH of the HMR solution
Alcohols				
Ethanol	–	0	n.a.[a]	5
Propan-2-ol	–	0	n.a.	5
Butan-2-ol	–	0	n.a.	5
Pentan-2-ol	–	0	n.a.	5
Ethanol in water, vol.%				
2	0	30	n.a.	5
Propan-2-ol in water, vol.%				
2	100	70	6	5
5	100	70	6	5
10	100	53	3	5
20	100	52	3	5
50	100	52	2	5
80	100	30	2	5
Butan-2-ol, vol.%				
2	0	30	n.a.	5
Pentan-2-ol, vol.%				
2	35[b]	65	9	5
Cyclohexanol, vol.%				
2	75[c]	24	0.2	5
Acetone, vol.%				
2	83[c]	15	0.1	5
1,4- Dioxane, vol.%				
2	100	44	1.3	5
80	100	15	0.6	6
100	-	0	n. a.	6
Tetrahydrofuran (THF), vol.%				
2	55	21	0.5	5
80	–	0	n. a.	5.5
100	–	0	n. a.	6

[a] n.a. = Not active in oxoMAT was formation. The main by-product was lignan.
[b] Conidendric acid (ConiA).
[c] Hydroxymatairesinol (HMR 1).

tion histogram, while magnesia has a bimodal one. The reason for such phenomena is the alkaline nature of magnesia. During the deposition, the pH increases due to the urea decomposition, which changes the charge of support surface. The rate of the gold precursor adsorption is linearly proportional to the difference between the pH value of media and the Point Zero Charge of the support (PZC), which is about 12 in case of magnesia [25]. Due to urea decomposition, the pH of media is increasing, which results in slow adsorption of gold complexes. At the same time, gold(III) chlorohydroxocomplexes tend to form gold(III) polynuclearhydroxocomplexes [26], which form agglomerates of gold particles in the solution and on the support surface. In case of slow adsorption,

Table 1
Dehydrogenation of HMR over Pd/C catalysts at 343 K under the nitrogen flow. Conditions: catalyst mass is corresponding to 5 mg of Pd mass, 100 mg of HMR, 100 ml of propan-2-ol.

Catalyst	Activity[a], $\times 10^4$ mol$_{oxoMAT}$/l $\times$ s $\times g_{Pd}$	Conversion after 4 h, %	Selectivity[b], %		Yield after 4 h, %	
			OxoMAT	MAT	OxoMAT	MAT
5 wt.% Pd/C (Degussa)	7.2	92	62	38	64.4	27.6
4 wt.% Pd/C (Sibunit)	5.3	87	87	13	73.1	13.9

[a] Activity of catalyst in the oxoMAT synthesis was calculated according to Eq. (3).
[b] Selectivity was calculated at 4% of HMR conversion.

(a) 2 wt.% Au/TiO$_2$ d = 1.9±1.0 nm

(b) 2 wt. % Au/SiO$_2$ d = 1.6±0.8 nm

(c) 2 wt.% Au/MgO   d = 2-3 nm and 6-8 nm

(d) 2.5 wt. % Au/C   d= 3.3 ± 1.2 nm
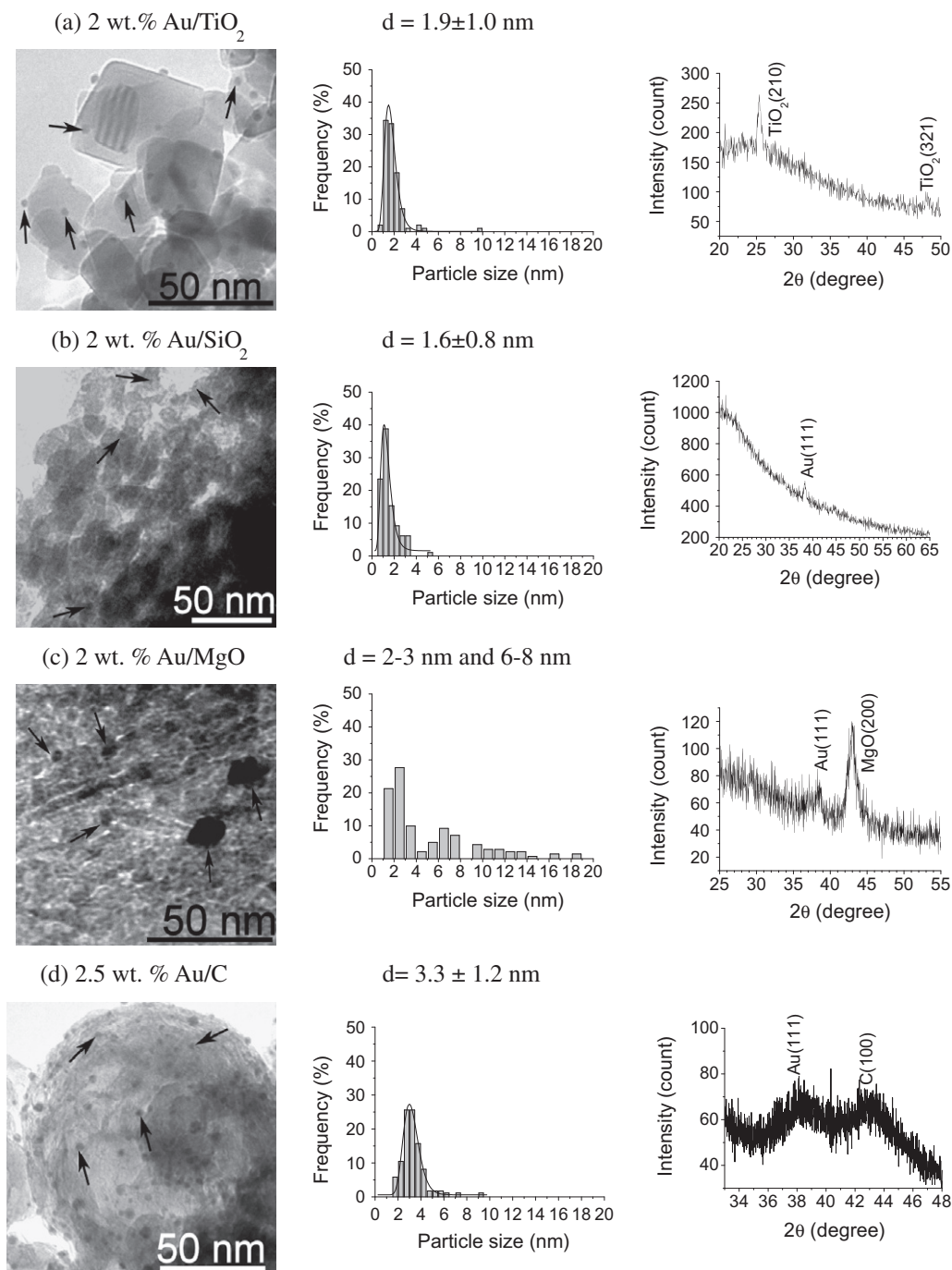
Fig. 2. TEM images and XRD patterns of the catalysts: (a) 2 wt.% Au/TiO$_2$; (b) 2 wt.% Au/SiO$_2$; (c) 2 wt.% Au/MgO; (d) 2.5 wt.% Au/C; (e) 2 wt.% Au/Al$_2$O$_3$-DIE; (f) 2 wt.% Au/Al$_2$O$_3$-DPU.

more gold(I) polynuclearhydroxocomplexes are formed in the solution followed by deposition of them onto magnesia surface as bigger particles.

The XRD results showed that in the most cases, Au reflections are missing indicating the presence of a very small gold particle size (less than 3 nm). Although an Au(1 1 1) reflection was observed in case of carbon and silica supports, the contribution of big particles is too small to be visible in the particle size distribution.

Pd catalyst supported on Sibunit has an average particle size 4.6 ± 2.2 nm. The catalyst Pd/C supplied by Degussa has a maximum in the particle size distribution at about 3 nm. XRD study has confirmed the results on the particle size obtained by TEM.

Gold loadings analyzed by ICP-OES are summarized in Table 3. The amount of supported gold was found to be in the range 1.4–2.4 wt.% depending on the support type.

3.1.2. Gold oxidation state

The X-ray photoelectron (XPS) spectra of the Au 4f core level of Au/Al$_2$O$_3$ catalysts show only one band corresponding to Au^0. However, in case of Au/TiO$_2$ and Au/SiO$_2$, the contribution of two metal states was detected: Au^0 and Au$^{\delta-}$. These observations could be explained by two phenomena: electron transfer from the support toward the gold particles [27,28] or a dominant effect of the atoms at low coordinated sites as proposed by Radnik and et al. [29]. The first one could be applied only to the titania supported

(e) 2 wt. % Au/Al$_2$O$_3$-DIE   d = 2.2 ± 1.1 nm

XRD is not reliable

(f) 2 wt. % Au/Al$_2$O$_3$-DPU   d = 2.3 ± 0.6 nm

XRD is not reliable
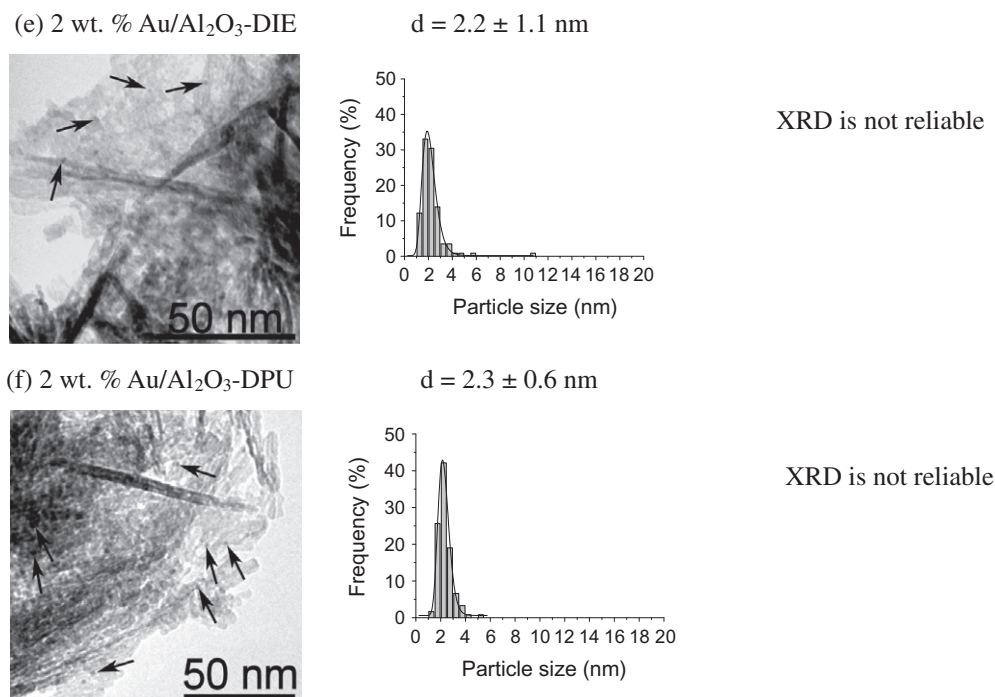
Fig. 2 (*continued*)

Table 3
Kinetic results on HMR oxidative dehydrogenation at 343 K under the synthetic air flow using 2 vol.% propan-2-ol in water as a solvent. Data was calculated according to Eqs. (1)–(3).

Entry	Catalyst	Metal loading, wt.%	Average Au particle size, nm	Activity, $\times 10^4$ mol$_{oxoMAT}$/ l $\times$ s $\times$ g$_{Au}$	Conversion of HMR after 240 min, %	Selectivity[a] to oxoMAT, %
1	Au/MgO	1.4 ± 0.10	2.0 ± 1.0	n.a.	100	0
2	Au/C	1.6 ± 0.60	3.3 ± 1.2	0.06	6	100 [b]
3	Au/SiO$_2$	2.4 ± 0.20	1.6 ± 0.8	5	13	100
4	Au/TiO$_2$	1.9 ± 0.20	1.9 ± 1.0	13	21	100
5	Au/Al$_2$O$_3$-DPU	2.0 ± 0.14	2.3 ± 0.6	23	50	100
6	Au/Al$_2$O$_3$-DIE	2.1 ± 0.15	2.2 ± 1.0	29	70	100
7	Al$_2$O$_3$	0	–	0	33	0 [c]
8	MgO	0	–	0	100	0 [c]

n.a. = Not active.
[a] Selectivity to oxoMAT was measured at 10% of HMR conversion.
[b] Selectivity was calculated at 6% of conversion.
[c] The product of the reaction over Al$_2$O$_3$ was HMR 1 and over MgO was ConiA.

catalyst, since silica demonstrates weak interactions with noble metal clusters [30]. The effect of low coordinated atoms could be detected in case of both carriers, silica and titania, since gold particle size is lower than 2 nm.

3.1.3. Support acidity and basicity
The nature of supports acid sites was studied by FTIR using pyridine as a probe molecule. Since Selli and Forni [31] have found a good correlation between the acidities obtained by FTIR measurements and those obtained by TPD for a number of different acidic catalysts, the pyridine FTIR technique can be applied for quantitative determination of acid sites. FTIR spectral interpretation was performed according to the commonly accepted procedure which attributes adsorption at about 1610 and 1450 cm^{-1} to Lewis acid sites and peaks at 1545 and 1630 cm^{-1} to pyridine adsorbed on Brønsted acid sites. Brønsted acidity was not observed in any of the samples, while the number of Lewis acid sites was different.

In order to study the alumina acidity and basicity changes during the catalyst preparation gold free, alumina support was treated in the same way as during the catalyst preparation by DIE (consequent washing with ammonia and water followed by drying and calcination). The obtained sample denoted as Al$_2$O$_3$-DIE was analyzed by pyridine FTIR and CO$_2$-TPD techniques.

Measurements on the acidity and basicity are collected in Table 4. Lewis acidity is increasing in the order: MgO = SiO$_2$ ≪ Al$_2$O$_3$-DIE < Al$_2$O$_3$ < TiO$_2$. The amount of alumina Lewis acid sites decreased during the treatment according to the catalyst preparation procedure. At the same time, the basicity of alumina before and after treatment was the same. Among the analyzed samples, magnesia possesses the highest basicity.

3.2. Catalytic results

Oxidative dehydrogenation of HMR was studied over different types of Pd and Au supported catalysts. Effects of different solvents

Table 4
Acidity and basicity of the supports.

Support	Acid sites (µmol/g)		Basic sites (µmol/g)	
	Brønsted	Lewis	Brønsted	Lewis
Al$_2$O$_3$	0	50	110	
Al$_2$O$_3$-DIE	0	10	110	
SiO$_2$	0	0	n.d.	
TiO$_2$	0	150	84	
MgO	0	0	250	

n.d. = Not determined.

and reaction atmospheres were studied over gold catalysts and compared with the performances over palladium catalysts.

Turn-over frequency, yield, and conversion were calculated as follows:

$$TOF = \frac{mol_{OxoMAT}^{20min}}{mol_{surfaceAu} \times 1200 \text{ s}} \tag{1}$$

TOF was calculated by dividing the initial reaction rate, calculated from the slope of the concentration–time plot, to the amount of exposed catalytic sites. The amount of surface Au was calculated according to the size of gold particles observed by TEM and catalyst metal loading.

$$Conversion = \frac{C_{HMR2}^0 - C_{HMR2}}{C_{HMR2}^0} \times 100\% \tag{2}$$

$$Activity = mol_{OxoMAT}/volume \times time_0 \times m_{cat} \tag{3}$$

3.2.1. Solvent effects

3.2.1.1. Palladium catalysts. HMR dehydrogenation over palladium catalysts was carried out at the same reaction conditions as described previously in [18]. Pd/Sibunit was tested using as a solvent propan-2-ol *per se* and 2 vol.% propan-2-ol in water. It was shown that the presence of water in the solvent significantly changes the catalyst activity and selectivity as well (Table 1). Palladium catalyst has higher activity applying propan-2ol *per se* as a solvent.

3.2.1.2. Gold catalysts. The oxidative dehydrogenation of HMR was performed in different solvents by using 2 wt.% Au/Al$_2$O$_3$ as a catalyst. Since HMR is poorly soluble in water and hydrocarbons, but well soluble in alcohols, the reaction was performed in different alcohols and their mixtures with water. In order to avoid the competitive oxidation of HMR and alcohols over the gold catalyst, the reaction was also performed using 1,4-dioxane and tetrahydrofuran (THF) and their mixtures with water as a solvent. Gold catalysts were not active in this reaction, when ethanol, propan-2-ol, butan-1-ol, pentan-2-ol were used as solvents. However, applying mixtures of alcohol and water as a solvent results in the formation of the desired product—oxoMAT. The formation of oxoMAT was also observed in solvents different from alcohols, e.g., 1,4-dioxane and tetrahydrofuran (THF) and their mixtures with water. Since the most probable by-products, Coni and ConiA, can be formed with increasing of the solution pH, the pH value of each reaction mixture was measured and found to be similar in all cases. Thus, the product distribution is not related to the difference in the solution pH. The results are presented in the Table 2.

Gold catalysts were inactive for the oxidative dehydrogenation of HMR, when pure alcohols were applied as solvents. However, application of alcohol with water mixtures results in oxoMAT formation due to HMR oxidative dehydrogenation. These changes could be related to the activity of gold catalysts in the alcohols oxidation [32,33]; thus, the catalyst interacts with the alcohol in the solvent rather than HMR. Alcohol can be oxidized over gold leading

to compounds, which are poisoning gold catalysts, as for example, acetone via propan-2-ol oxidation [34] or other aldehydes and carboxylic acids generated from corresponding alcohol. The formation of acetone from propan-2-ol was detected in the present work by using high-performance liquid chromatography (HPLC), analysis procedure is described in [35]. Thus, when an alcohol–water mixture was applied, gold catalysts became active in the oxoMAT synthesis due to a minor effect of alcohols oxidation. Moreover, the catalytic activity is increasing with the increasing water content in the reaction mixture. The highest activity and selectivity were reached applying 2 and 5 vol.% propan-2-ol in water as a solvent.

Utilization of cyclohexanol–water mixture as a solvent was an attempt to diminish the contribution of solvent oxidation via steric hindrance [36]. Application of this solvent resulted in lower catalytic activity and selectivity to oxidation/dehydrogenation reaction compared with propan-2-ol–water mixture.

In order to investigate the effect of acetone, which could be formed during the reaction as a by-product due to oxidation of propan-2-ol from the solvent, the reaction was performed in acetone–water solution. Although the content of acetone was only 2 vol.%, the activity of the catalyst dramatically decreased. The selectivity toward desired oxoMAT was 83%, while the less active isomer HMR 1 was also produced.

To exclude the competitive oxidation of alcohol from the solvent and the reactant HMR, solvents such as 1,4-dioxane and THF were utilized. Application of these solvents showed that the catalyst was becoming more active with increasing of water content in the solution. No HMR oxidation/dehydrogenation to oxoMAT in pure 1,4-dioxane and THF was detected. This result could be explained by further transformation of these solvents on the catalyst active sites in reactions such as ring opening, consequent oxidation and polymerization [37–39].

The selective aerobic oxidation of HMR was studied using a range of organic solvents and their mixtures with water. It was observed that increasing water content in the reaction mixture resulted in increasing conversion of HMR to the desired product—oxoMAT. The same tendency was discovered in [40], where water had shown to have a promotion effect on the activity of gold catalyst. In case of HMR oxidation, the role of water could be related to two phenomena: first, suppressing of described above possible deactivation due to organic solvent interaction with catalyst surface and second, activation of adsorbed oxygen by adsorbed water, due to formation of hydroperoxyl-like intermediate species (OOH) followed by their decomposition and releasing of O* and H$_2$O [37].

3.2.2. Effect of catalysts: active metal, support and preparation method

3.2.2.1. Palladium catalysts. The tested Pd/C catalysts have shown different catalytic behavior (Table 1) with the highest activity achieved over 5 wt.% Pd/C (Degussa), which could be associated with larger support acidity [18]. Conversion of HMR over Pd/C (Degussa) after 4 h was similar to the case of Pd on Sibunit supported catalysts.

Over palladium catalysts HMR undergoes two types of transformation: dehydrogenation to oxoMAT and hydrogenolysis to MAT [18]. The studied Pd catalysts have shown different selectivity toward these products (Table 1). In particular, selectivity and yield of oxoMAT were the highest in case of Pd/C (Sibunit) catalyst. The reaction kinetics over this catalyst is shown in Fig. 3. The increasing of HMR 1 concentration in the beginning of the reaction was related to the isomerization of HMR 2 to HMR 1.

3.2.2.2. Gold catalysts.

3.2.2.2.1. Catalytic activity. The tested gold catalysts have shown different activities toward oxidation/dehydrogenation of HMR (Table 3). Among the catalysts active in selective HMR oxidation/dehydrogenation, the most active catalyst was gold supported on
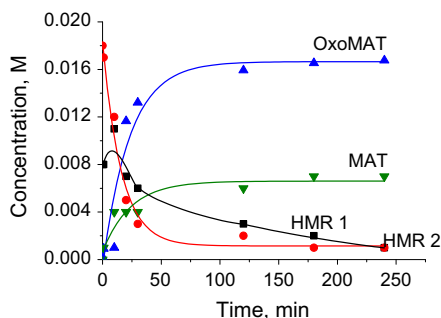
Fig. 3. Transformation of HMR to oxoMAT and MAT over Pd/C (Sibunit) catalyst under nitrogen flow at 343 K in propan-2-ol.

alumina (Table 3, entry 6). The reaction over titania and silica supported catalysts resulted in relatively low yields of HMR (entries 3 and 4, Table 3). The lowest activity was obtained over the carbon supported gold catalyst. As was already studied in [18], in case of palladium, catalysts with a higher support acidity had higher activity in dehydration. The same tendency was detected in case of the gold catalysts. The acidity of the carbon supported catalyst cannot be measured by the same technique as applied for metal oxides, e.g., pyridine desorption studied by FTIR. However, the acidity of carbons is typically lower than those of metal oxides. The obtained data on carbon supported gold catalyst showed the lowest activity in the HMR transformation. The gold catalysts supported on different metal oxides exhibited the following trend in TOF for the HMR transformation: $MgO \ll SiO_2 < Al_2O_3$ (Table 3), which follows the same order of increasing Lewis acidities (Table 4). It is worth to note that although titania possesses higher acidity than applied alumina, the activity of Au/TiO_2 is lower. This difference could be attributed to the different state of the supported gold ($Au^{\delta-}$), detected by XPS, and related to the strong metal-support interaction.

The HMR oxidation reaction is in fact selective oxidation of secondary alcohols. TOF of oxoMAT synthesis over gold catalysts was changing in the range 1×10^{-3} s^{-1} to 20×10^{-3} s^{-1}, which is much lower than TOF values calculated for other secondary alcohols oxidation reaction over supported gold [41]. This difference could be related to the steric hindrance of OH-group in HMR presented in different conformations [42].

The alumina supported gold catalysts displayed metal particle size distributions, measured by TEM and XRD techniques that were independent of the preparation method; however, their activity was different. Since the methods of catalysts preparation, namely DPU and DIE, have different mechanisms of gold particles deposition; consequently, the gold particles size distribution could be different. The DPU method allows formation of $[Au(Cl)_{4-x}(OH)_x]^-$ complexes [43] and their growth on the support surface similarly as in the water solution, forming polymeric gold (III) chlorohydroxocomplexes [26] during the deposition procedure. The other method used for gold deposition on the alumina surface, DIE, implies the adsorption of hydrolyzed gold precursor as $[Au(Cl)_{4-x}(OH)_x]^-$ followed by ammonia washing, which efficiently removes the remaining chloride ions [20]. Thus, it was supposed that DIE method results in formation of smaller particles not visible either by TEM or detected by XRD techniques. This assumption could explain the difference in the activity of the tested catalysts supported on alumina, while more active catalyst is prepared by DIE method resulting in supposedly higher dispersion of gold catalysts.

3.2.2.2.2. Activity. Gold catalysts have shown different activity in the reaction of oxoMAT synthesis. The rate constants for the HMR transformation reaction were calculated assuming the kinetic curve described by the first order kinetics. The results are presented in the Table 5.

The conversion of HMR was the highest with Au/MgO, but this catalyst was not selective to oxoMAT (Table 3). The conversion of HMR over other Au supported catalysts increases with increasing of supports acidity (Table 4).

Furthermore, the Au/Al$_2$O$_3$-DIE catalyst was more active than Au/Al$_2$O$_3$-DPU giving after 240 min 70% conversion, whereas only 50% conversion was achieved over the latter catalyst.

Moreover, both supports, alumina and magnesia, without supported gold particles were active in the HMR isomerization (Table 3, entries 7 and 8). However, no oxoMAT was formed in the absence of gold, thus, indicating that the presence of gold particles is needed for the synthesis of the desired product—oxoMAT.

3.2.2.2.3. Yield and selectivity. Except magnesia supported gold catalyst, all the catalysts displayed 100% selectivity toward oxoMAT, while Pd catalysts tested in [18] and described in this paper have shown lower selectivity toward oxoMAT.

In the case of Au/MgO catalysts, HMR was transformed into another lignans: conidendrin (Coni) and conidendric acid (ConiA) (see Fig. 1) by HMR dehydration followed by cyclization. This behavior is related to the basicity of magnesia, as ConiA is normally formed with increasing pH value of the solution.

The isomers of HMR, HMR 1 and HMR 2, can be transformed into each other. At the same time, there was no isomerization observed over gold catalysts active in HMR oxidation. As was already mentioned, alumina *per se* was active in the isomerisation of HMR 2 to HMR 1. However, under the same reaction conditions, alumina supported gold particles were able to change the reaction selectivity toward oxoMAT formation.

The dependence of the oxoMAT yield on time for all the tested catalysts is shown in Fig. 4. The yield and conversion were calculated according to Eqs. (2) and (3).

The yield of oxoMAT was found to be dependent on the catalyst support. Since oxoMAT was the only product of HMR oxidative dehydrogenation, the yield of oxoMAT is increasing in the same order as catalysts activity: $MgO \ll SiO_2 < TiO_2 < Al_2O_3$ (Table 3). According to the shape of the curves presented on the Fig. 3, during

Table 5
Calculated reaction rate constants.

Catalyst	$k \times 10^2$, s$^{-1} \times g_{Au}^{-1}$
2 wt.% Au/Al$_2$O$_3$-DIE	6.4 ± 0.8
2 wt.% Au/Al$_2$O$_3$-DPU	5.4 ± 0.4
2 wt.% Au/TiO$_2$	5.0 ± 0.2
2 wt.% Au/SiO$_2$	4.0 ± 0.4
2 wt.% Au/C	0.4 ± 0.04
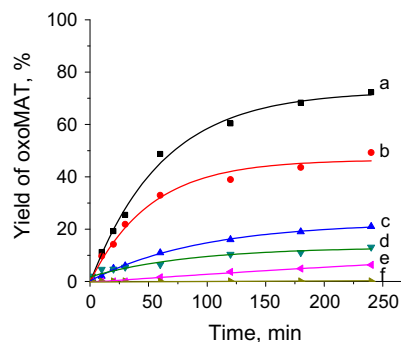
Fig. 4. OxoMAT yield as a function of time at 343 K using 2 vol.% propan-2-ol in water as a solvent in air flow over 250 mg catalysts: (a) Au/Al$_2$O$_3$-DIE (d = 2.2 ± 1.0 nm); (b) Au/Al$_2$O$_3$-DPU (d = 2.3 ± 0.6 nm); (c) Au/TiO$_2$ (d = 1.9 ± 1.0 nm); (d) Au/SiO$_2$(d = 1.6 ± 0.8 nm); (e) Au/C (d = 3.3 ± 1.2 nm); (f) Au/MgO (d = 2.0 ± 1.0 nm and 7.0 ± 1.0 nm).
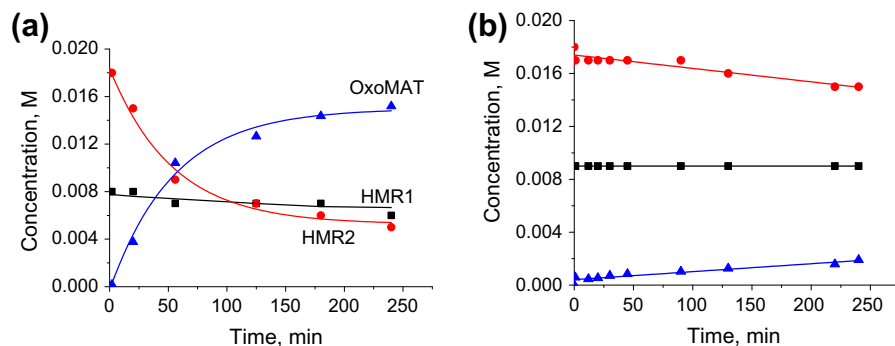
Fig. 5. Dehydrogenation of HMR in 2 vol.% propan-2-ol in water over 250 mg of 2 wt.% Au/Al$_2$O$_3$-DIE catalyst at 343 K under the flow of: (a) synthetic air; (b) nitrogen.
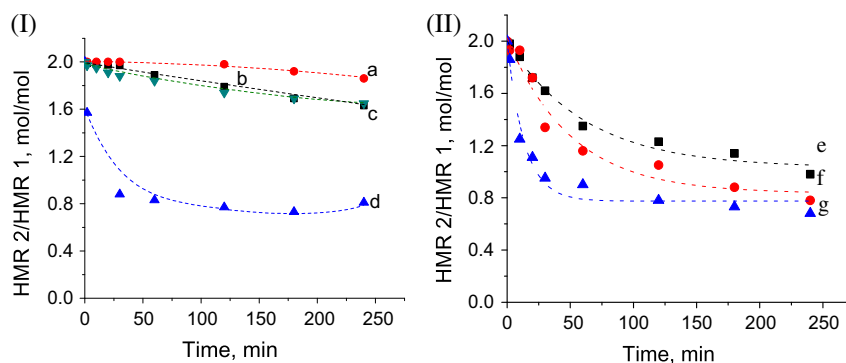
Fig. 6. Ratio HMR 2/HMR 1 vs. the reaction time of the HMR oxidative dehydrogenation reaction in 2 vol.% propan-2-ol in water in air flow at 70 °C over 250 mg of: I—a)Au/C; (b) Au/TiO$_2$; (c) Au/SiO$_2$; (d) Au/MgO; II—(e) Au/Al$_2$O$_3$-DPU; (f) Au/Al$_2$O$_3$-DIE; (g) Al$_2$O$_3$.

the reaction, the deactivation is taking place most probably due to stronger adsorption of oxidation products than reactants. It should be explicitly mentioned that Au/MgO displayed zero activity toward oxoMAT formation, although Fig. 4 might give a wrong impression due to the properties of graphical software.

3.2.3. Effect of the reaction atmosphere

3.2.3.1. Palladium catalysts.
Applied Pd/C catalysts were not active in the presence of oxygen (under the air flow). Thus, all the further described results were obtained under the flowing nitrogen in line with previous workers [18]. The reason for such behavior is that Pd catalysts could be deactivated in the presence of oxygen due to Pd oxide formation, which is catalytically not active.

3.2.3.2. Gold catalysts.
Since oxoMAT formation was observed over Pd catalysts under the nitrogen flow, activities of gold catalysts in the oxoMAT synthesis were studied under the same reaction conditions in the absence of oxygen. The kinetic curves shown in the Fig. 5 clearly demonstrate that the presence of oxygen significant increases the catalyst activity.

The HMR conversion over Au/Al$_2$O$_3$-DIE was 17% after 4 h under nitrogen atmosphere (Fig. 5b), whereas under oxygen, the conversion was much higher being 68% (Fig. 5a). The selectivity toward oxoMAT was 100% in both cases: in the absence and presence of oxygen. These results confirmed that the HMR transformation over gold includes the dehydrogenation route, not requiring presence of oxygen.

It was already reported that gold catalysts have catalytic activity in the reaction of alcohols oxidation in the absence of oxygen. However, the presence of oxygen leads to removing of adsorbed hydrogen atoms by co-adsorbed oxygen [44], thus, increasing the reaction rate.

3.2.4. Reactivity of HMR 1 and HMR 2 over gold

In case of the applications of the gold catalysts described in this paper, no isomerization between HMR 1 and HMR 2 was observed. However, the molar ratio between these two isomers changes differently during the reaction, dependent on the catalyst. The results were also compared with the activity of the alumina support without gold particles, since alumina catalyzes the isomerization of HMR 2 to HMR 1 as presented on Fig. 6.

Two isomers, HMR 1 and HMR 2, have different reactivity in oxidative dehydrogenation. As was already mentioned, HMR 2 is the only isomer transformed in the most cases, while in case of the highly active alumina supported gold catalyst prepared by DIE, HMR 1 was also oxidized to oxoMAT (Fig. 7a). Comparison of the catalytic behavior of the alumina support and Au/Al$_2$O$_3$ toward the HMR transformation (Fig. 5a and 8) showed explicitly the activity of alumina toward the isomerization of HMR 2 to HMR 1. The conversion of HMR 2 after 4 h was 33%, giving exclusively HMR 1 as a product. Thus, HMR 1 consumption during the oxidation could be either from isomerization of HMR 2 or oxidative dehydrogenation to oxoMAT. In order to investigate the routes of HMR isomers transformation, the reaction was performed using the isolated isomers HMR 1 and HMR 2 separately as starting materials under the same conditions as for their mixture over Au/Al$_2$O$_3$-DIE catalyst.

Procedure of gold catalyst preparation could suppress the activity of alumina toward isomerization HMR 2 to HMR 1 due to support acidity changing (Table 4). The adsorption of alcohols on alumina surface takes place due to interactions with Lewis acid site (Al) and Brønsted base site as studied in [45]. HMR hydroxyl-group interactions with alumina surface can be described in the same way as secondary alcohols adsorption on alumina. Thus, the following explanation could be proposed: due to the decreasing
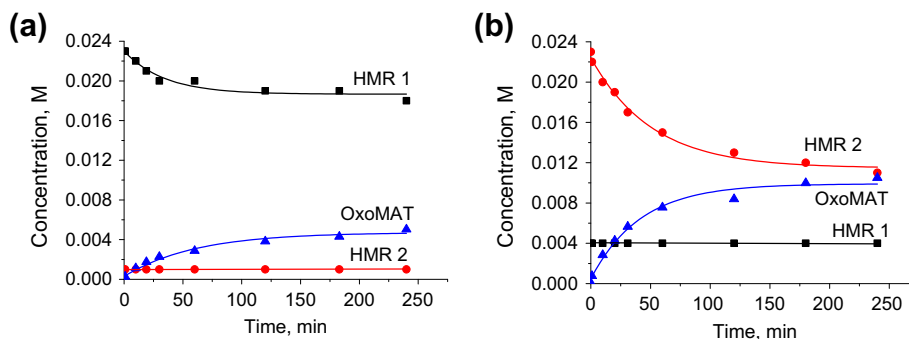
Fig. 7. Kinetic results on the oxidation/dehydrogenation of: (a) HMR 1; (b) HMR 2 over Au/Al$_2$O$_3$-DIE catalyst at 343 K in 2 vol.% propan-2-ol in water under synthetic air flow.
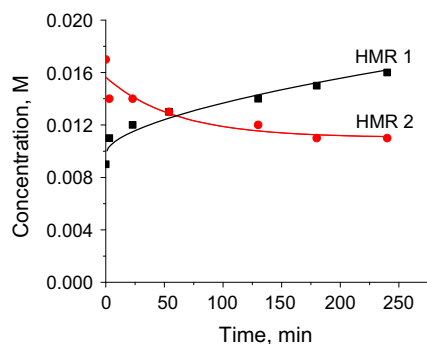
Fig. 8. Concentration vs. time dependency of HMR transformation in 2 vol.% propan-2-ol in water under synthetic air flow at 70 °C over 245 mg of Al$_2$O$_3$.

amount of Lewis acid sites the isomerization reaction is suppressed, while oxidation of HMR is taking place via the adsorption on the gold surface followed by alkoxy-intermediate formation [41].

The obtained kinetic curves (Fig. 7) demonstrate that both isomers oxidized to oxoMAT and no isomerization to each other was observed. However, isomer HMR 1 is less active, than HMR 2, reaching only 17% of conversion after 4 h, while during the same time, HMR 2 is converted to 52% extent. These results support the assumption that conversion of HMR 1 in the mixture with HMR 2 is related to the oxidation of this isomer to oxoMAT.

Dehydrogenation of the isolated isomers over Pd/C catalysts was studied previously. The isomer HMR 2 also reacted with higher reaction rate. Quantum chemical calculations had showed that HMR 1 formed more stable intermediate than HMR 2, therefore, rendering it less active [18]. The same explanations could probably be used in case of the reaction over gold catalysts.

4. Conclusions

Gold catalysts were for the first time studied in oxidative dehydrogenation of a lignan, hydroxymatairesinol (HMR) to another lignan, oxomatairesinol (oxoMAT), which is a promising antioxidant and anticarcinogenic compound for pharmaceutical and cosmetic products, as well as a color-keeping agent in textile industry. Despite a complicated chemical structure of the substrate, the reaction in essence is a transformation of secondary alcohol to a corresponding ketone. Activity and selectivity of gold catalysts were compared with those of palladium catalysts which exhibited selectivity to oxomatairesinol (oxoMAT) of 70%. Investigation of the reaction showed that the activity of utilized gold catalysts strongly depends on several parameters, such as the catalyst support, gold oxidation state, solvent, and gaseous atmosphere.

Activity of gold catalysts is high in the solvent containing mainly water when oxygen is used as an oxidizing agent.

Palladium catalysts exhibited high catalyst activity only in propan-2-ol and under a nitrogen atmosphere. Contrary to palladium, gold catalysts were not active either in propan-2-ol or other studied organic solvents and exhibited lower activity in the absence of oxygen than in aerobic conditions. In addition, application of gold catalysts afforded 100% selectivity toward the desired product.

Hydroxymatairesinol (HMR) was applied as a mixture of two diastereomers of HMR: (7R,8R,8'R)-(-)-7-allo-hydroxymatairesinol (HMR 1) and (7S,8R,8'R)-(-)-7-allo-hydroxymatairesinol (HMR 2), which can be isomerized into each other. HMR isomers have different activity toward oxomatairesinol (oxoMAT) synthesis, which can be explained by different adsorption strength of diastereomers. Such assumption requires further theoretical investigation by quantum chemical methods, which is now in progress.

References

[1] N.M. Saarinen, A. Smeds, S.I. Makela, C. Eckerman, M. Reunanen, M. Ahotupa, S.M. Salmi, A.A. Franke, L. Kangas, R. Santti, Nutr Cancer 36 (2000) 207.
[2] R. Ekman, Holzforschung 30 (1976) 79.
[3] S. Willför, P. Eklund, R. Sjöholm, M. Reunanen, R. Sillanpää, S. von Schoultz, J. Hemming, L. Nisula, B. Holmbom, Holzforschung 59 (4) (2005) 413.
[4] P.C. Eklund, S. Willför, A. Smeds, B.R. Holmbom, R.E. Sjöholm, J. Nat. Prod. 67 (6) (2004) 927.
[5] S. Willför, J. Hemming, M. Reunanen, C. Eckerman, B. Holmbom, Holzforschung 57 (2003) 27.
[6] H. Adlercreutz, Phytoestrogens and human health, in: K. Korach (Ed.), Reproductive and Developmental Toxicology, Marcel & Dekker, NY, 1998, pp. 299–371.
[7] S.M. Willför, M.O. Ahotupa, J.E. Hemming, M.H.T. Reunanen, P.C. Eklund, R.E. Sjöholm, C.S.E. Eckerman, S.P. Pohjamo, B.R. Holmbom, J. Agr. Food Chem. 51 (2003) 7600.
[8] S. Yamaguchi, T. Sugahara, Y. Nakashima, A. Okada, K. Akiyama, T. Kishida, M. Maruyama, T. Masuda, Biosci. Biotechnol. Biochem. 70 (2006) 1934.
[9] P.C. Eklund, O.K. Långvik, J.P. Wärnå, T.O. Salmi, S.M. Willför, R.E. Sjöholm, Org. Biomol. Chem. 3 (2005) 3336.
[10] H. Korte, M. Unkila, M. Hiilovaara-Teijo, V.-M. Lehtola, M. Ahotupa, Patent WO/2004/000304 A1, 2003.
[11] T. Ahlnäs, Patent WO 2008/020112 A1, 2008.
[12] P. Eklund, R. Sillanpää, R. Sjöholm, J. Chem. Soc. Perkin Trans. 1 (2002) 1906.
[13] P.C. Eklund, R.E. Sjöholm, Tetrahedron 59 (2003) 4515.
[14] P. Eklund, A. Lindholm, J.-P. Mikkola, A. Smeds, R. Lehtilal, R. Sjöholm, Org. Lett. 5 (2003) 491.
[15] R. Sjöholm, P. Eklund, J.-P. Mikkola, R. Lehtila, M. Sodervale, A. Kalapudas, US Patent 0080299, 2005.
[16] F. Kawamura, M. Miyachi, S. Kaway, J. Wood Sci. 44 (1998) 47.

[17] P. Eklund, A. Lindholm, J.-P. Mikkola, A. Smeds, R. Lehtilä, R. Sjöholm, Org. Lett. 5 (4) (2003) 491.
[18] H. Markus, A.J. Plomp, T. Sandberg, V. Nieminen, J.H. Bitter, D.Yu. Murzin, J. Mol. Catal. A. 274 (2007) 42.
[19] O.A. Simakova, P.A. Simonov, A.V. Romanenko, I.L. Simakova, React. Kinet. Catal. Lett. 95 (1) (2008) 3.
[20] S. Ivanova, V. Pitchon, Y. Zimmermann, C. Petit, Appl. Catal. A 298 (2006) 57.
[21] E.V. Murzina, A.V. Tokarev, K. Kordás, H. Karhu, J.-P. Mikkola, D.Yu. Murzin, Catal. Today 131 (2008) 385.
[22] F. Porta, L. Prati, M. Rossi, S. Coluccia, G. Martra, Catal. Today 61 (2000) 165.
[23] M. Zaki, M. Hasan, F.A. Al-Sagheer, L. Pasupulety, Colloids Surf. A 190 (2001) 261.
[24] H. Markus, P. Mäki-Arvela, N. Kumar, N.V. Kul'kova, P. Eklund, R. Sjöhölm, B. Holmbom, T. Salmi, D.Yu. Murzin, Catal. Lett. 103 (2005) 125.
[25] S. Ardizzone, C.L. Bianchi, B. Vercelli, Colloids Surf. A 144 (1–3) (1998) 9.
[26] P.A. Simonov, V.A. Likholobov, in: A. Wieckowski, E.R. Savinova, C.G. Vayenas (Eds.), Catalysis and Electrocatalysis at Nanoparticle Surfaces, Marcel Dekker, New York, 2003, p. 409.
[27] P. Claus, A. Bruückner, C. Mohr, H. Hofmeister, J. Am. Chem. Soc. 122 (11) (2000) 430.
[28] A. Sanchez, S. Abbet, U. Heiz, W.-D. Schneider, H. Häkkinen, R.N. Barnett, U. Landman, J. Phys. Chem. A 103 (1999) 9573.
[29] J. Radnik, C. Mohr, P. Claus, Phys. Chem. Chem. Phys. 5 (2003) 172.
[30] G.C. Bond, in: B. Imelik, C. Naccache, G. Courier, H. Praliaud, P. Meriaudeau, P. Gallezot, G.A. Martin, J.C. Vedrine (Eds.), Metal-Support and Metal Additive Effects in Catalysis, Elsevier, Amsterdam, 1982 (Chapter 1).
[31] E. Selli, L. Forni, Micropor. Mesopor. Mater. 31 (1999) 129.
[32] L. Prati, F. Porta, Appl. Catal. A 291 (1–2) (2005) 199.
[33] S. Demirel, P. Kern, M. Lucas, P. Claus, Catal. Today 122 (3–4) (2007) 292.
[34] J. Gong, D.W. Flaherty, T. Yan, C.B. Mullins, ChemPhysChem 9 (17) (2008) 2461.
[35] M. Käldström, N. Kumar, T. Heikkilä, M. Titta, T. Salmi, D.Yu. Murzin, ChemCatChem 2 (5) (2010) 539.
[36] J. Clayden, N. Greeves, S. Warren, P. Wothers, Organic Chemistry, Oxford University Press, Oxford, 2000. p. 1508.
[37] H. Liang, H. Gao, Q. Kong, Z. Chen, J. Chem. Eng. Data 51 (2006) 119.
[38] M. Sommovigo, H. Alper, J. Mol. Catal. 88 (1994) 151.
[39] A. Aouissi, S.S. Al-Deyab, H. Al-Shahri, Molecules 15 (2010) 1398.
[40] X. Yang, X. Wang, C. Liang, W. Su, C. Wang, Z. Feng, C. Li, J. Qiu, Catal. Commun. 9 (2008) 2278.
[41] A. Abad, C. Almela, A. Corma, H. Garcia, Tetrahedron 62 (2006) 6666.
[42] A. Taskinen, P. Eklund, R. Sjöholm, M. Hotokka, J. Mol. Catal. A 333 (2010) 136.
[43] F. Moreau, G.C. Bond, A.O. Taylor, J. Catal. 231 (2005) 105.
[44] Y. Guan, E.J.M. Hensen, Appl. Catal. A 361 (2009) 49.
[45] S. Cai, K. Sohlberg, J. Mol. Catal. A 193 (2003) 157.